



Article Info

Received: 11th August 2023Revised: 18th December 2023Accepted: 20th December 2023

Department of Chemistry, Ibrahim
Badamasi Babangida University Lapai,
Niger State Nigeria

*Corresponding author's email:

johntsadom@gmail.com;jmathew@ibbu.edu.ngCite this: *CaJoST*, 2024, 1, 26-34

Development of Fe₃O₄ Nanoparticles for the Removal of Some Toxic Metals from Pharmaceutical Wastewater

John T. Mathew*, Monday Musah, Yakubu Azeh and Musa Mohammed

Among the most significant sources of environmental contamination are pharmaceutical wastewaters, which are often contaminated with heavy metals that pose significant threats to ecosystems as well as public health. The nanoparticles was characterized using XRD, HRSEM/EDX and FTIR. The XRD analysis of the nanoparticles identified 2θ (theta), of 30.2°, 36.3°, 44.2°, 54.3°, 58.2°, 63.5°, and 74.6° which correspond to the crystal lattice planes of (220), (311), (400), (422), (511), (440), and (533), respectively. The diffraction peaks associated with Fe₃O₄ at 2θ of 18.02°, 29.4°, and 43.3°, related to the crystal planes of (111), (220), and (400), respectively of the Fe₃O₄ phase. The HRSEM image of the nanoparticles exhibited spherical-shaped structures of Fe₃O₄, and some irregular shapes. The effects of the dosage; consequently, the impact of the quantity of adsorbent used, ranging from 0.1 to 0.3 g, has been investigated. The results indicate that as the amount of adsorbent is increased from 0.1 to 0.3 g, the effectiveness of adsorption improves, while temperature, the efficiency improved from 50.03% to 78.01% for Pb ions, from 52.15% to 82.43% for Cd ions, and from 56.41% to 88.71% for Cu ions and contact time; the removal efficiency for Pb ions rises from 25.49% to 68.43%, for Cd ions from 29.30% to 75.71%, and for Cu ions from 31.08% to 78.31%, respectively, on the removal percentage of toxic metal ions were studied.. This research offers a sustainable and eco-friendly solution to mitigate toxic metal contamination in pharmaceutical effluents, protecting the environment and human well-being while advancing the field of wastewater treatment.

Keywords: Environmental, Heavy, Langmuir, Metal, Nanocomposites, Pharmaceutical, Wastewater.

1. Introduction

In the wake of industrialization and rapid population growth, the pharmaceutical industry has witnessed unprecedented expansion, contributing to enhanced healthcare but also generating a significant environmental concern – pharmaceutical wastewater (Mathew et al., 2024). This wastewater is laden with diverse contaminants, including various toxic metals (Pd, Cu, Cd, Pb and Cr), which can pose substantial threats to both the environment and human health (Okoro et al. 2023). The removal of these toxic metals from pharmaceutical wastewater has thus become an imperative challenge. To address this concern, the development and application of advanced nanoadsorbents have garnered attention as an innovative and sustainable solution (Inobeme et al. 2023a). Among these nanoadsorbents, iron oxide nanoparticles, particularly Fe₃O₄ nanoparticles, have emerged as a promising candidate for efficient and eco-friendly removal of toxic metals

from pharmaceutical effluents (Kumar et al., 2021).

Pharmaceutical wastewater contains a complex mixture of organic and inorganic contaminants, including various toxic metals, which pose a significant environmental and human health risk when released into natural water bodies (Inobeme et al. 2023b). The presence of toxic metals in pharmaceutical effluents is primarily due to their incorporation in drug formulations and the manufacturing processes. In recent years, the need for effective and sustainable treatment methods to remove these hazardous contaminants has gained considerable attention (Hejna et al. 2022).

Among various treatment strategies, the utilization of nanomaterials for adsorption has emerged as a promising and environmentally friendly approach for the removal of toxic metals from wastewater (Adetunji et al. 2022).

Nanoadsorbents, particularly iron oxide nanoparticles (e.g., Fe₃O₄), have shown exceptional potential in the efficient and cost-effective removal of heavy metals. Their unique characteristics, such as high surface area, tunable surface chemistry, and superparamagnetic properties, make them well-suited for wastewater treatment applications (Ethaib et al. 2022).

The selected toxic metals may include but are not limited to lead (Pb), cadmium (Cd), and copper (Cu), all of which are known to have detrimental effects on the environment and human health (Mathew et al. 2022). The aim of this research is to explore the efficiency, selectivity, and practicality of Fe₃O₄ nanoparticles as an innovative and eco-friendly solution for addressing the challenge of toxic metal removal from pharmaceutical wastewater (Elnabi et al. 2023; Inobeme et al. 2023c). By investigating the feasibility and efficacy of Fe₃O₄ nanoparticles as nanoadsorbents, this study contributes to the growing body of knowledge in the field of wastewater treatment and environmental remediation, offering a sustainable solution to the critical issue of toxic metal (Pb, Cd and Cu) contamination in pharmaceutical effluents.

2. Materials and Methods

2.1 Synthesis of Fe₃O₄ nanoparticles

A 10.0 g of Fe(NO₃)₃ was dissolved in 100 cm³ of deionized water in a 250 cm³ beaker under a continuous stirring using a magnetic stirrer. 0.1 M sodium hydroxide (NaOH) was added to the mixture to maintain a pH of 10. The precipitated nanoparticles were copiously washed with ethanol and deionized water. After thorough washing, the nanoparticles were dried in an oven at 105 °C for 24 h and further calcined at 450 °C for 3 h (Thoda et al., 2023).

2.2 Characterization of nanomaterials

2.2.1 X-ray diffraction (XRD)

The samples were characterized using Bruker AXS D8 Advance X-ray diffractometer with Cu K α radiation to determine the phase and crystallite size. The powdered sample was placed on the aluminium sample holder, the diffractograms were recorded in the 2 theta range of 20° to 90° and phase identification was investigated (Mathew et al., 2023c).

2.2.2 Resolution transmission electron microscopy (HRTEM)

The morphology and structure of the sample were characterized using Zeiss Auriga High-resolution transmission electron microscopy (HRTEM). The synthesized sample (0.02 g) was suspended in 10 cm³ of methanol and ultrasonicated until complete dispersion was

achieved. Two drops of suspension were dropped onto a holey carbon grid with the help of micropipette and later dried through exposure to photo light.

2.2.3 High-resolution scanning electron microscopy (HRSEM)

The morphologies of the materials were investigated using Zeiss Auriga high-resolution scanning electron microscopy. The sample (0.05 mg) was sprinkled onto carbon adhesive tape and sputter coated with Au-Pd using Quorum T150T Analyzer for 5 min. The coated sample was loaded in the sample holder and operated with high electron tension at 5 kV for imaging (Mathew et al., 2023a).

2.2.4 Fourier transform infra-red spectroscopy

FTIR spectra of the samples were recorded using a Perkin-Elmer 2000 FTIR spectrometer fitted with a deuterated triglycine sulphate (DTGS) detector covering the frequency range of 500-4000 cm⁻¹. Ten milligrams (0.01 g) of the dried samples were evenly dispersed in 200 mg of spectroscopic grade KBr to record the spectra. The sample spectra were recorded in 500 to 4000 cm⁻¹ wavenumbers (Mathew et al., 2023b).

2.3 Heavy Metal Determination

About 50 cm³ of the wastewater sample was measured into a 100 cm³ beaker with the addition of 15 cm³ concentrated trioxonitrate (V) solution and 10 cm³ of 50 % concentrated hydrochloric acid. The contents were heated on a hot plate and 7 cm³ of 50 % concentrated hydrochloric acid added and heated for 10 min. The solution was allowed to cool, and then deionized water was added and filtered into a 100 cm³ Pyrex volumetric flask using Whatman No 42 filter paper. This was then made up to the mark with deionized water and stored for further analysis of toxic metals such as Cd, Pb and Cu using AAS (Perkin Elmer 200 Atomic Absorption Spectrophotometer) (Sumaila et al. 2016; Adamu et al. 2017).

2.4 Batch Adsorption Processes

Batch equilibrium adsorption experiments were performed in order to evaluate the equilibrium time, obtain adsorption kinetics, adsorption isotherm and adsorption thermodynamic data. The removal efficiency (% removal) and the adsorption capacity, q_e (mg/g) of some physical and chemical indicators from tannery wastewater solution by adsorbents at different conditions were calculated using equations 1 and 2.

The adsorption capacities of the differently prepared adsorbents were determined as follows:

$$\% \text{ removal} = \frac{C_0 - C_e}{C_0} \times 100 \quad (1)$$

$$q_e = \frac{(C_0 - C_e)}{M} V \quad (2)$$

where C_0 (mg/dm^3) and C_e (mg/dm^3) are the initial and equilibrium liquid phase concentration, respectively; V (dm^3) the volume of the solution and M (g) the mass of the adsorbent.

The adsorption experiments were designed to carry out the adsorption characteristics of the beneficiated clay and nanocomposites under various conditions. The effects of parameters such as contact time, mass ratio of adsorbent to the volume of adsorbate and temperature on some indicator parameters were determined (Musah *et al.*, 2022).

2.4.1 Effect of contact time

The effects of contact time on the physical and chemical indicators analysed in this research using the adsorbents were investigated by contacting 0.20 g of the adsorbents in each case, with 100 cm^3 of the wastewater in a corked 250 cm^3 conical flask, agitated at 150 rotations per min (rpm) for 0, 5, 10, 15, 20, and 25 min on an orbital shaker. The samples were analysed after filtration by Whatman No. 42 filter paper. The final concentrations of metal ions were analysed using atomic absorption spectrometer (AAS). The optimum contact time, especially for the adsorbents for metal ions sorption from wastewater were also determined (Musah *et al.*, 2022).

2.4.2 Effect of adsorbent dose

The effects of adsorbent dosage on the equilibrium uptake of physical and chemical indicators from wastewater using adsorbents were investigated with adsorbent doses of 0.4, 0.6, 0.8, 1.0, 1.2 and 1.4 g, respectively. The experiments were performed by adding the known weights of the adsorbents into 250 cm^3 flasks containing 100 cm^3 of the wastewater each. The flasks were shaken at 150 rpm at the optimum contact time of each adsorbent. The samples were filtered using Whatman paper No. 42 and the concentrations of the metal ions were measured using atomic absorption spectrometer (AAS).

2.4.3 Effect of temperature

The effects of temperature on the equilibrium uptake of the indicator parameters from tannery wastewater by adsorbents at the temperature values of 30, 40, 50, 60, 70 and 80 $^\circ\text{C}$ were investigated. The experiments were performed by adding 0.2 g of the adsorbent to 100 cm^3 of wastewater in 250 cm^3 conical flasks. The corked flasks were shaken in a water bath at respective temperature for the optimum contact time. The samples were filtered using Whatman paper No. 42 and the concentrations of metal ions were measured using atomic absorption spectrometer (AAS).

3. Results and Discussion

The X-ray diffraction (XRD) pattern of the Fe_3O_4 nanoparticles that were synthesized and then subjected to a calcination process at 450 $^\circ\text{C}$ is depicted in Fig. 1. The diffraction lines that were obtained are located at specific angles corresponding to the crystal lattice planes of (220), (311), (400), (422), (511), (440), and (533). These lines closely match those expected for the tetragonal structure of magnetite (Fe_3O_4), as indicated by the reference data in the JCPDS database under file 25-1402. A similar outcome was also documented by Alamier *et al.* (2022). It's important to note that some magnetite nanoparticles might contain species of maghemite, a related material. However, distinguishing the standard diffraction reflections of these species can be challenging due to their similarities. To estimate the crystal size of the Fe_3O_4 nanoparticles, the Debye-Scherrer equation (1) was utilized.

$$D = \frac{k\lambda}{\beta \cos\theta} \quad (1)$$

where D is the average Fe_3O_4 nanoparticle size, 0.89 is Scherrer's constant, 1.54 is the X-ray wavelength, β is half of the maximum intensity, and θ is Bragg's diffraction angle. The mean crystallite size of the Fe_3O_4 NPs is 20.09 nm.

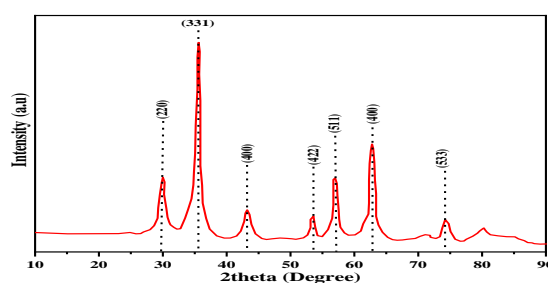


Fig 1: XRD result of Fe_3O_4 nanoparticles

The physical characteristics of the synthesized Fe_3O_4 nanoparticles were examined through SEM, as illustrated in Fig. 2. The SEM image

indicates that the Fe₃O₄ nanoparticles exhibit a spherical morphology and are interconnected, leading to the formation of clusters. This clustering phenomenon might be attributed to the inherent magnetic properties of the material, which causes them to attract and cluster together. Furthermore, the SEM analysis also reveals that the adsorbent has a porous structure. This structural porosity plays a significant role in improving the efficiency of the adsorption process.

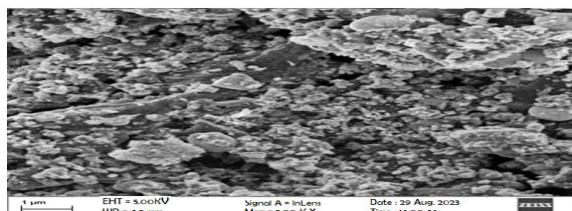


Fig. 2: SEM image of Fe₃O₄ nanoparticles

EDX analysis confirms the presence of iron (Fe) and oxygen (O) in the sample, which are the constituents of Fe₃O₄ (Fig. 3). This confirms the formation of the desired iron oxide nanoparticles.

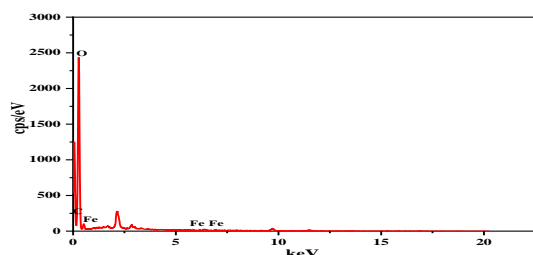


Fig. 3: EDX spectrum of Fe₃O₄ nanoparticles

The study involved an exploration of (FTIR) analysis to discern the distinctive characteristics of surface functional groups present in Fe₃O₄ nanoparticles. The FTIR spectrum for the produced Fe₃O₄ nanoparticles is illustrated in Fig. 4. The spectrum displays various peaks that provide insights into the molecular bonds and functional groups within the sample. The wide peak observed at 3590 cm⁻¹ indicates the stretching vibration of O-H bonds, representing hydroxyl (OH) groups. The smaller peak at 2949 cm⁻¹ corresponds to stretching vibrations of -CH₂ groups. Furthermore, peaks at 1790 cm⁻¹ and 1340 cm⁻¹ relate to bending and asymmetric vibrations of C-H bonds, specifically capturing the characteristics of carbon-hydrogen bonds. A peak at 1148 cm⁻¹ signifies the stretching of C-O bonds, representing the presence of carbonyl (C=O) groups. Observing the FTIR spectrum, additional peaks at 900 cm⁻¹ suggest C-H bending vibrations, underlining the presence of carbon-hydrogen bonds. Peaks appearing at 620 cm⁻¹ provide evidence of the successful synthesis of Fe₃O₄ nanoparticles through the Fe-O stretching vibration mode. Finally, a peak at

578 cm⁻¹ can be attributed to the stretching vibration of metal-oxygen bonds, specifically signifying the presence of metals at tetrahedral sites.

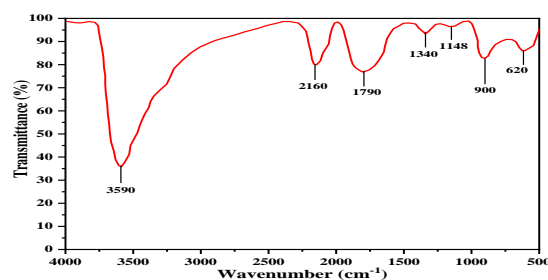


Fig. 4: FTIR spectrum of Fe₃O₄ nanoparticles

3.1 Effect of contact time

The impact of the duration of contact (ranging from 0 to 30 min) on the process of adsorbing metal ions using Fe₃O₄ nanoparticles has been depicted in Fig. 5. The data illustrates that the efficiency of removing these metal ions increases as the contact time lengthens, eventually stabilizing at 25 min for the removal of Pb, Cd, and Cu ions from wastewater. The initial rapid rise in the adsorption percentage is attributed to the abundance of available binding sites on the adsorbent surface for the metal ions to attach. This outcome is expected, as initially, there are numerous sites accessible for the adsorption of metal ions.

However, over time, the remaining vacant surface sites become harder to occupy due to the repulsive forces between the metal ions present in the solid phase and those in the surrounding mass phase, as pointed out by Choudhury et al. (2022). Consequently, the proportion of metal ions that can be removed increases significantly. Specifically, the removal efficiency for Pb ions rises from 25.49% to 68.43%, for Cd ions from 29.30% to 75.71%, and for Cu ions from 31.08% to 78.31%, respectively. Upon analyzing the percentage removal of metal ions over different contact times, it becomes evident that Cu(II) ions exhibit a higher tendency to be adsorbed onto Fe₃O₄ nanoparticles compared to Pb(II) and Cd(II) ions.

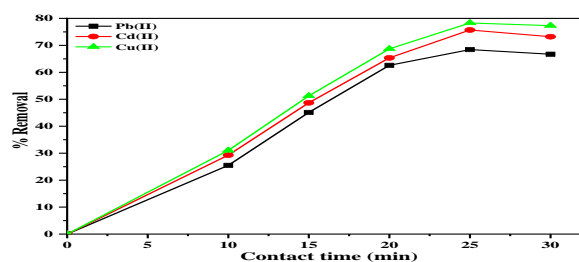


Fig. 5: Effect of contact time on the removal of heavy metal ions

3.2 Effect of adsorbent dose

The amount of adsorbent used is another crucial and highly influential factor that significantly impacts the process of adsorption and the capacity of adsorption. Consequently, the impact of the quantity of adsorbent used, ranging from 0.1 to 0.3 g, has been investigated. The results indicate that as the amount of adsorbent is increased from 0.1 to 0.3 g, the effectiveness of adsorption improves: for Pb ions, the removal efficiency increases from 75.42% to 98.60%; for Cd ions, it goes from 80.10% to 99.10%; and for Cu ions, it rises from 86.04% to 100% (as illustrated in Fig. 6). This enhancement in the percentage of metal ion removal can be attributed to an expanded adsorption surface area and a greater number of available sites for adsorption, as pointed out by Song *et al.* (2021). With the escalation in adsorbent dosage, more active sites become accessible for binding metal ions, resulting in an augmentation of adsorption efficiency until saturation is reached.

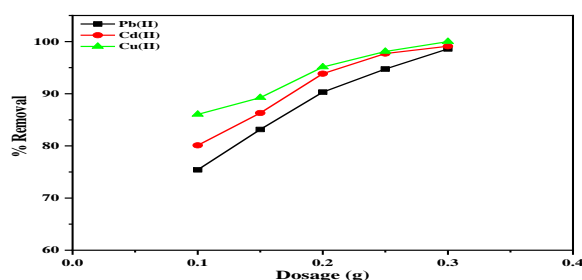


Fig. 6: Effect of dosage on the removal of heavy metal ions

3.3 Effect of temperature

The temperature of a solution significantly influences the adsorption process, especially in removing pollutants. Experiments were conducted at various temperatures to investigate this phenomenon, as illustrated in Fig. 7. The outcomes demonstrated a noteworthy trend. When the temperature was elevated from 30 to 80°C, there was a noticeable increase in the maximum adsorption efficiency. For instance, the efficiency improved from 50.03% to 78.01% for Pb ions, from 52.15% to 82.43% for Cd ions, and from 56.41% to 88.71% for Cu ions. This temperature-dependent enhancement in adsorption efficiency indicates that adsorbing metal ions onto Fe₃O₄ nanoparticles is driven by an input of heat; in other words, it is an endothermic process. This observation aligns with the findings of Mahanty *et al.* (2020). This phenomenon can be attributed to the higher temperatures facilitating the movement and penetration of metal ions within the porous structure of the Fe₃O₄ nanoparticles. As the temperature rises, the kinetic energy of the metal ions increases, allowing them to navigate the

pores of the adsorbent material better. This increased mobility overcomes the energy barrier, known as activation energy that metal ions need to surpass to be adsorbed. Therefore, the adsorption capacity of Fe₃O₄ nanoparticles is notably improved at elevated temperatures due to the augmented motion and infiltration of metal ions within the adsorbent's porous framework.

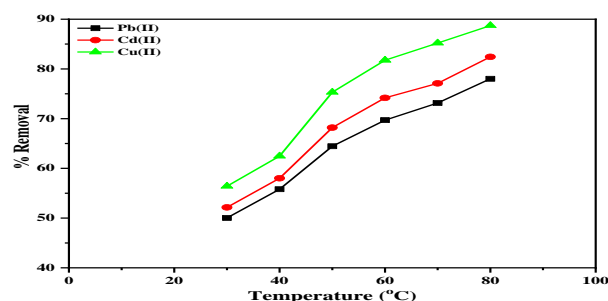


Fig. 7: Effect of temperature on the removal of heavy metal ions

3.4 Adsorption isotherm

Adsorption isotherms serve as important tools for describing the connection between the equilibrium capacity of an adsorbent (the substance doing the adsorbing) and the adsorbate (the substance being adsorbed), offering valuable insights into the adsorption process (Musah *et al.* 2022). This investigation focused on studying the Langmuir and Freundlich adsorption isotherms at various temperatures, as detailed in Table 1. The Langmuir model assumes that all available adsorption sites possess identical characteristics and that the adsorbate forms a monolayer on the even and uniform surface of the adsorbent. On the other hand, the Freundlich model is commonly employed when the adsorbent's surface is uneven or heterogeneous. The equations that define these isotherm models are provided below;

$$\frac{C_e}{q_e} = \frac{1}{bq_m} + \frac{C_e}{q_m} \quad (2)$$

$$\ln q_e = \ln K_f + \frac{1}{n} \ln C_e \quad (3)$$

where C_e is the equilibrium concentration of substrates in the solution (mg/dm³), q_e is the adsorption capacity at equilibrium (mg/g), q_m is the maximum adsorption capacity (mg/g) and b is the adsorption equilibrium constant (L/mg). K_f and n are known as Freundlich constants, and they play important roles in describing the adsorption process. The parameter 'n' offers insights into the level of favorability of the adsorption process. On the other hand, ' K_f ' (measured in milligrams per gram, mg/g) quantifies the maximum adsorption capacity of the adsorbent material. The specific values for these parameters can be found in Table 1.

Among the various models used to understand adsorption phenomena, the Langmuir model's results stood out. This was particularly evident through the R² values, which indicate how well the experimental data matches the model's predictions. In all instances, the R² values for the Langmuir model were consistently the highest, surpassing 0.988. This outcome strongly suggests that the Langmuir model offers the most appropriate and accurate description for the adsorption processes of metal ions onto Fe₃O₄ nanoparticles.

Table 1: Isotherm models of metal ions removal in wastewater

Isotherm	Parameter	Pb(II)	Cd(II)	Cu(II)
Langmuir	K_L	0.0038	0.0042	0.0051
	Q_m	87.10	101.89	128.07
	R^2	0.9821	0.9886	0.9942
Freundlich	K_f	0.341	2.705	4.126
	n	0.386	0.612	0.782
	R^2	0.9682	0.9805	0.9826

3.5 Adsorption kinetic

The kinetics of adsorption plays a crucial role in assessing the effectiveness of an adsorbent. It characterizes how quickly a solute is taken up by the adsorbent material, governing the rate at which molecules diffuse and the duration they spend adhered to the solid-solution interface. In evaluating how well Fe₃O₄ nanoparticles work as an adsorbent, two commonly used kinetic models—the pseudo-first-order and pseudo-second-order models—were employed to analyze the experimental findings. The data in Table 2 outlines the kinetic parameters for the adsorption of Pb, Cd, and Cu ions.

Upon analyzing the results, it is evident that the pseudo-second-order model offers a better description of the adsorption process using Fe₃O₄ nanoparticles for all tested metal ions, as indicated by its higher correlation coefficient (R²). This suggests that the chemisorption process predominantly controls the adsorption, as discussed by Xu et al. (2022). In terms of removing metal ions, the outcomes highlight that the rate constant for Cu²⁺ (1.063 g mg⁻¹ min⁻¹) surpasses the rate constants for Pb²⁺ (0.784 g mg⁻¹ min⁻¹) and Cd²⁺ (0.902 g mg⁻¹ min⁻¹). This underscores the strong affinity of Fe₃O₄ nanoparticles for Cu²⁺ ions and demonstrates their rapid migration in scenarios involving competitive adsorption within multi-component wastewater systems.

Table 2: Kinetic models of metal ions removal in wastewater

Kinetic	Parameter	Pb(II)	Cd(II)	Cu(II)
Pseudo-first-order	k_1	0.0186	0.0236	0.0682
	q_e	45.081	59.013	69.106
	R^2	0.8422	0.8479	0.8616
Pseudo-second-order	k_2	0.784	0.902	1.063
	q_e	91.208	106.258	110.519
	R^2	0.9237	0.9709	0.9890

3.6 Thermodynamic study

Thermodynamics of metal ions adsorbed onto Fe₃O₄ nanoparticles was investigated at 30 to 80 °C, and the thermodynamic parameters (Gibbs free energy change (ΔG°, kJ mol⁻¹), enthalpy change (ΔH°, kJ mol⁻¹) and entropy change (ΔS°, J mol⁻¹ K⁻¹) were calculated using Eqs. (4-6).

$$K_d = \frac{q_e}{C_e} \quad (4)$$

$$\Delta G = -RT \ln K_d \quad (5)$$

$$\Delta G = \Delta H - T\Delta S \quad (6)$$

where the values of ΔG, ΔH, and ΔS were measured in kJ/mol, kJ/mol, and J/molK respectively. T is the absolute temperature (K), R is the universal gas constant (8.314 J/molK), K_d value is obtained by plotting $\ln\left(\frac{q_e}{C_e}\right)$ against C_e (Shaba et al. 2019).

The findings presented in Table 3 indicate that the change in enthalpy associated with the adsorption of metal ions onto Fe₃O₄ nanoparticles is positive. This positive enthalpy change suggests that the adsorption process is endothermic, requiring energy input from the surroundings. This phenomenon can be attributed to the strong interaction between the Fe₃O₄ nanoparticles and the metal ions. Essentially, the process of adsorption is facilitated by the absorption of heat. The positive entropy change value signifies an increase in disorder or randomness at the interface between the solid (Fe₃O₄ nanoparticles) and the solution (metal ions) during adsorption. This enhanced entropy can be linked to structural alterations within the Fe₃O₄ nanoparticles and the metal ions as they come into contact and bind together. This supports the notion that the adsorption process contributes to an increase in the overall disorder of the system. As indicated in Table 6, the ΔG° values were consistently negative for all cases, indicating that the adsorption processes of the metal ions onto the Fe₃O₄ nanoparticles occurred spontaneously. This aligns with the fact that

these adsorption events were energetically favorable and did not require external energy input to take place (Wen *et al.*, 2022).

Furthermore, the negative trend in the ΔG° values with increasing temperature implies that the adsorption of contaminants onto Fe_3O_4 nanoparticles became more favorable at higher temperatures. In other words, elevated temperatures made it easier for the nanoparticles to remove the metal ions from the solution. This could be attributed to the fact that higher temperatures expedited the hydration of metal ions, thereby facilitating their interaction with the nanoparticles and subsequent removal from the solution (Patel, 2020). The positive values of both ΔH° (enthalpy change) and ΔS° (entropy change) further emphasize that the adsorption process is endothermic and that the interface between the adsorbent and the wastewater becomes more disordered during the process. The rise in ΔG° with increasing temperature leads to greater adsorption, especially since higher temperatures promote faster hydration of metal ions, enhancing their adsorption onto the nanoparticles.

Table 3: Thermodynamic study of metal ions removal in wastewater

Parameter	Temperature (°C)	ΔS (kJ/mol \cdot K)	ΔH (kJ/mol)	ΔG (kJ/mol)
Pb(II)	30	21.15	72.08	-0.69024
	40	21.15	72.08	-1.41104
	50	21.15	72.08	-2.13184
	60	21.15	72.08	-2.85264
	70	21.15	72.08	-3.57344
	80	21.15	72.08	-4.29424
Cd(II)	30	20.15	71.73	-1.58419
	40	20.15	71.73	-2.30149
	50	20.15	71.73	-3.01879
	60	20.15	71.73	-3.73609
	70	20.15	71.73	-4.45339
	80	20.15	71.73	-5.17069
Cu(II)	30	19.96	72.09	-1.88327
	40	19.96	72.09	-2.60417
	50	19.96	72.09	-3.32507
	60	19.96	72.09	-4.04597
	70	19.96	72.09	-4.76687
	80	19.96	72.09	-5.48777

4. Conclusion

The utilization of Fe_3O_4 nanoparticles as nanoadsorbents for the removal of selected toxic metals from pharmaceutical wastewater

has shown significant promise. This research has demonstrated the potential of Fe_3O_4 nanoparticles to efficiently adsorb toxic metals, including lead, cadmium, arsenic, mercury, and chromium, from complex pharmaceutical wastewater matrices. The adsorption mechanisms governing the interaction between Fe_3O_4 nanoparticles and toxic metals have been elucidated, providing valuable insights into the underlying processes. The practical applicability of this technology has been explored, demonstrating its potential for scaling up to address the wastewater treatment needs of the pharmaceutical industry. This research contributes to the advancement of sustainable and efficient solutions for the removal of toxic metals from pharmaceutical wastewater, aligning with the principles of environmental protection and industrial compliance. Fe_3O_4 nanoparticles offer a viable path towards a cleaner, safer, and more environmentally responsible pharmaceutical manufacturing process.

Conflict of interest

The authors declare no conflict of interest.

Acknowledgements

In appreciation for funding this study, the authors are grateful to the Tertiary Education Trust Fund (TETFund) and the management of IBB University, Lapai for fostering an enabling research environment.

References

- Adamu A., Iyaka Y. A., Mathew J. T., Inobeme A. and Egharevba H. O. (2017). Assessment of Some Heavy Metal Contamination and analysis of Physicochemical Parameters of Surface Soil within the Vicinity of Minna Railway Station, Niger State, Nigeria. *Journal of Applied Life Sciences International*, 10(1), 1-9. doi: 10.9734/JALSI/2017/28671
- Adetunji, C. O., Ogundolie F. A., Ajiboye, M. D., Mathew, J. T., Inobeme, A., Olotu T., Olaniyan, O., Ijabadeniyi, O. A., Ajayi, O. O., Dauda, W. P., Ghazanfar, S., and Adetunji, J. B. (2022). Bio- and Nanosensors in the Food Industry. In a book: Bio- and Nano-sensing Technologies for Food Processing and Packaging, The Royal Society of Chemistry, 22-36. doi:10.1039/9781839167966-00022.
- Alamier, W. M., El-Moselhy, M. M., Bakry, A. M., Hasan, N., & Alamri, A. A. (2022). Biogenic Synthesis of Zero Valent Fe/Magnetite Fe_3O_4 Nanoparticles Using *Caralluma acutangula* and Application for Methylene Blue Dye

- Degradation under UV Light Irradiation. *Crystals*, 12(11), 1510. doi.org/10.3390/cryst12111510.
- Choudhury, T.R., Rahman, M.S., Liba, S.I., Islam, A., Quraishi, S.B., Begum, B.A., Mustafa, A.I. and Amin, M.N., 2022. Adsorptive removal of chromium from aqueous solutions using flax (*Linum usitatissimum*): Kinetics and equilibrium studies. *Environmental Chemistry and Ecotoxicology*, 4, pp.132-139. doi.org/10.1016/j.enceco.2022.02.004
- Elnabi, A. M. K., Elkaliny, N. E., Elyazied, M. M., Azab, S. H., Elkhalifa, S. A., Elmasry, S., Mouhamed, M. S., Shalamesh, E. M., Alhoriény, N. A., Abd Elaty, A. E., Elgendy, I. M., Etman, A. E., Saad, K. E., Tsigkou, K., Ali, S. S., Kornaros, M., & Mahmoud, Y. A.-G. (2023). Toxicity of Heavy Metals and Recent Advances in Their Removal: A Review. *Toxics*, 11(7), 580. https://doi.org/10.3390/toxics11070580.
- Ethaib, S., Al-Qutaifia, S., Al-Ansari, N., & Zubaidi, S. L. (2022). Function of Nanomaterials in Removing Heavy Metals for Water and Wastewater Remediation: A Review. *Environments*, 9(10), 123. doi.org/10.3390/toxics11070580
- Hejna, M., Kapuścińska, D., & Aksmann, A. (2022). Pharmaceuticals in the Aquatic Environment: A Review on Eco-Toxicology and the Remediation Potential of Algae. *International journal of environmental research and public health*, 19(13), 7717. doi: 10.3390/ijerph19137717
- Inobeme, A., Adetunji, C. O., Mathew, J T., Ajai, A. I., Inobeme, J., Bamigboye, M. O., Onyeaku, S., Maliki, M., Eziukwu, C. & Tawa, K. (2023a). Nanotechnology for Bioremediation of Heavy Metals. In book: *Microbial Technologies in Industrial Wastewater Treatment*. Springer Nature Singapore, 19-30. https://doi.org/10.1007/978-981-99-2435-6_2.
- Inobeme, A., Adetunji, C. O., Maliki, M., Onyeaku, B. I., Kelani, T., Eziukwu, C. A., Olori, E., Mathew, J. T., and Bamigboye, M. O. (2023b). Strategies to synthesize, advantages, and disadvantages of pharmaceutical nanoparticles. In book: *Nanotechnology for Drug Delivery and Pharmaceuticals*. Academic Press is an imprint of Elsevier, 371-402. doi: https://doi.org/10.1016/B978-0-323-95325-2.00006-7.
- Inobeme, A., Adetunji, C. O., Mathew, J. T., Okonkwo, S., Bamigboye, M. O., Ajai, A. I., Afoso, E. and Inobeme, J. (2023c). Advanced nanotechnology for the degradation of persistent organic pollutants. In: Shah, M. ed. *Microbial Degradation and Detoxification of Pollutants*. Berlin, Boston: De Gruyter, pp. 51-72. https://doi.org/10.1515/9783110743623-003
- Kumar, R., Rauwel, P., & Rauwel, E. (2021). Nanoadsorbants for the Removal of Heavy Metals from Contaminated Water: Current Scenario and Future Directions. *Processes*, 9(8), 1379. https://doi.org/10.3390/pr9081379
- Mahanty, S., Chatterjee, S., Ghosh, S., Tudu, P., Gaine, T., Bakshi, M., Das, S., Das, P., Bhattacharyya, S., Bandyopadhyay, S. and Chaudhuri, P., (2020). Synergistic approach towards the sustainable management of heavy metals in wastewater using mycosynthesized iron oxide nanoparticles: Biofabrication, adsorptive dynamics and chemometric modeling study. *Journal of Water Process Engineering*, 37, p.101426. https://doi.org/10.1016/j.jwpe.2020.101426.
- Mathew, J. T., Inobeme, A., Musah, M., Azeh, Y., Abdullahi, A., Shaba E. Y., Salihu, A. M., Muhammad, E. B., Josiah, J. G., Jibrin, N. A., Ismail, H., Muhammad, A. I., Maurice, J., Mamman, A. & Ndamitso, M. M. (2024). A Critical Review of Green Approach on Wastewater Treatment Strategies. *Journal of Applied Science and Environmental Management*, 28(2), 363-391. doi: https://dx.doi.org/10.4314/jasem.v28i2.9
- Mathew, J. T., Musah, M., Azeh, Y. and Muhammed, M. (2023a). Adsorptive Removal of Selected Toxic Metals from Pharmaceutical Wastewater using Fe₃O₄/ZnO Nanocomposite, *Dutse Journal of Pure and Applied Sciences*, 9(4a), 236- 248. https://dx.doi.org/10.4314/dujopas.v9i4a.22.
- Mathew, J. T., Adetunji, C. O., Inobeme, A., Musah, M., Azeh, Y., Otori, A.A., Shaba, E. Y., Mamman, A. and Tanko, E. (2023b). Removal of Heavy Metals Using Bio-remedial Techniques. Springer Nature Switzerland AG 2023 M. P. Shah (ed.), *Modern Approaches in Waste Bioremediation*, 117-130. https://doi.org/10.1007/978-3-031-24086-7_6.
- Mathew, J. T., Musah, M., Azeh, Y. & Muhammed, M. (2023c). Kinetic Study of Heavy Metals Removal from Pharmaceutical Wastewater Using Geopolymer/Fe₃O₄ Nanocomposite. *Bima Journal of Science and Technology*, 7(4), 152- 163. Doi: 10.56892/bima.v7i4.539.
- Mathew, J. T., Adetunji, C. O., Inobeme, A., Musah, M., Shaba, E. Y., Azeh, Y., Abulude, F. O. and Mamman, A. (2022). Organic Compounds in Atmospheric Aerosols: Atmospheric Aerosols Properties, Sources and Detection. Nova Science Publishers, Inc. 43-59. doi.org/10.52305/CXUG8701

- Musah, M., Azeh, Y., Mathew, J. T., Umar, M.T., Abdulhamid, Z. & Muhammad, A. I. (2022). Adsorption Kinetics and Isotherm Models: A Review. *Caliphate Journal of Science & Technology*, 1, 20-26. Doi: <https://doi.org/10.4314/cajost.v4i1.3>.
- Okoro, H.K., Orosun, M.M., Oriade, F.A., Momoh-Salami, T.M., Ogunkunle, C.O., Adeniyi, A.G., Zvinowanda, C. & Ngila, J.C. (2023). Potentially Toxic Elements in Pharmaceutical Industrial Effluents: A Review on Risk Assessment, Treatment, and Management for Human Health. *Sustainability*, 15, 6974. doi: 10.3390/su15086974.
- Patel, H. (2020). Batch and continuous fixed bed adsorption of heavy metals removal using activated charcoal from neem (*Azadirachta indica*) leaf powder. *Scientific Reports*, 10(1), 16895. <https://doi.org/10.1038/s41598-020-72583-6>
- Shaba, E.Y., Mathew, J.T, Musah, M., and Agboba, E.I. (2019). The Kinetic and Thermodynamic Study of the Removal of Selected heavy Metals from a Nigerian Brewery Wastewater Using Activated Carbon From Cheese Wood (*alstonia boonei*). "Theme: Sustainable Energy in hanging limate: The Role of Science and Technology", in 2nd School of Physical Sciences Biennial International Conference Futminna 2019, on 24th -27th June, Minna, Niger State.
- Song, X., Cao, Y., Bu, X., & Luo, X. (2021). Porous vaterite and cubic calcite aggregated calcium carbonate obtained from steamed ammonia liquid waste for Cu²⁺ heavy metal ions removal by adsorption process. *Applied Surface Science*, 536, 147958. <https://doi.org/10.1016/j.apsusc.2020.147958>
- Sumaila A. Enochel D. E. Mathew J. T. and Okaraga A. S. (2016). Synthesis and Characterization of Prymethamine-Sulphadoxine Metal Complexes. *African Journal of Science and Research*. 1(5), 63 – 66.
- Wen, Y., Xie, Z., Xue, S., Long, J., Shi, W., & Liu, Y. (2022). Preparation of novel polymethacryloyl hydrazone modified sodium alginate porous adsorbent with good stability and selective adsorption capacity towards metal ions. *Separation and Purification Technology*, 303, 122184. <https://doi.org/10.1016/j.seppur.2022.122184>.
- Xu, X., Zhang, M., Lv, H., Zhou, Y., Yang, Y., & Yu, D. G. (2022). Electrospun polyacrylonitrile-based lace nanostructures and their Cu (II) adsorption. *Separation and Purification Technology*, 288, 120643. <https://doi.org/10.1016/j.seppur.2022.120643>